Atmos. Meas. Tech. Discuss., 7, 293–320, 2014
www.atmos-meas-tech-discuss.net/7/293/2014/
doi:10.5194/amtd-7-293-2014

Atmospheric Measurement Techniques Discussions

Interference of sulphur dioxide to balloon-borne ECC ozone sensors over the Valley of Mexico

I. Kanda[1], R. Basaldud[2], N. Horikoshi[3], Y. Okazaki[1], S. E. Benítez Garcia[1], A. Ortínez[2], V. R. Ramos Benítez[4], B. Cárdenas[2], and S. Wakamatsu[1]

[1]Ehime University, Matsuyama, Ehime, Japan
[2]Mexico National Institute of Ecology and Climate Change (INECC), DF, Mexico City, Mexico
[3]Meteoric Research Inc., Tokyo, Japan
[4]Mexico National Weather Service (SMN), DF, Mexico

Received: 22 November 2013 – Accepted: 18 December 2013 – Published: 15 January 2014

Correspondence to: I. Kanda (ikanda@agr.ehime-u.ac.jp)

Published by Copernicus Publications on behalf of the European Geosciences Union.

Abstract

Abnormal decrease in the ozonesonde sensor signal occurred during air-pollution study campaigns in November 2011 and March 2012 in Mexico City. Sharp drops around 5 km a.s.l. and above were observed in November 2011, and a broad deficit in the convective boundary layer in March 2012. Various circumstantial evidence indicates that the decrease was due to interference of SO_2 gas to Electrochemical Concentration Cell (ECC) ozone sensors. The sharp drops in November 2011 are considered to be caused by the SO_2 plume from the Popocatépetl volcano to the south-east of Mexico City. Response experiments of the ECC sensor to representative atmospheric trace gases showed that only SO_2 could generate the observed abrupt drops. The vertical structure of the plume reproduced by a Lagrangian particle diffusion simulation also supported this assumption. The near-ground deficit in March 2012 is considered to be generated by the SO_2 plume from the Tula industrial complex to the north-west of Mexico City. Sporadic large SO_2 emission is known to occur from this region, and before and at the ozonesonde launching time, large intermittent peaks of SO_2 concentration were recorded at the ground-level monitoring stations. The difference between the O_3 concentration obtained by ozonesonde and that by UV-based O_3 monitor was consistent with the SO_2 concentration measured by a UV-based monitor on the ground. The plume vertical profiles estimated by the Lagrangian particle diffusion simulation agreed fairly well with the observed profile. Statistical analysis of the wind field in Mexico City revealed that the Popocatépetl effect is most likely to occur from June to October, and the Tula effect all the year.

1 Introduction

Ozone (O_3) concentration in Mexico City frequently exceeds the environmental standard although the overall level has decreased substantially since around 1992 when the city was regarded as one of the most polluted megacities in the world (Mage et al.,

AMTD
7, 293–320, 2014

1996). High levels of O_3 concentration occur in urban areas because O_3 is produced by photochemical reactions involving nitrogen oxides and volatile organic compounds that are emitted mainly by anthropogenic activities (e.g., Seinfeld and Pandis, 2006). Tropospheric O_3 has negative effects on our lives if its concentration is exceedingly high; it causes health problems such as sore throat, uncomfortable breathing, and increased asthma attacks, it reduces crop yields and causes forest decline by damaging the leaves, and further it has a potential to change the global climate with its strong radiative forcing.

In Mexico City or in Mexico City Metropolitan Area (MCMA) (Fig. 1), many studies have been conducted to understand the life cycle of O_3: its production, transport, chemical reaction, and destruction. Although more difficult to obtain than the horizontal distribution, vertical profiles of O_3 concentration are essential in the understanding because O_3 produced near the ground and that existing at high concentration in the stratosphere are transported both horizontally and vertically by atmospheric motions of wide range of spatial and temporal scales. In past studies, vertical profiles of O_3 over MCMA were measured using airplanes (Emmons et al., 2010), tethered balloons (Velasco et al., 2008), and ozonesondes (Thompson et al., 2008). Airplane measurements up to about 10 km above sea level (hereinafter called a.s.l.) and extending horizontally over a spatial scale of the Mexico territory were used to validate a global chemical transport model MOZART-4. Tethered balloon measurements revealed the diurnal cycle of O_3 in the lower part ($\lesssim$ 800 m above ground level (hereinafter called a.g.l.)) of the planetary boundary layer. Ozonesonde measurements up to about 35 km a.s.l. focused on the long-range transport in the upper troposphere. In our study, ozonesonde was used mainly to obtain the vertical profiles of O_3 in the lower to upper troposphere.

Ozonesonde measurement employing liquid-phase reaction of potassium iodide (KI) and O_3 is known to be affected by the presence of sulphur dioxide (SO_2): one molecule of SO_2 entering the reaction cell eliminates the output electric current that would be generated by one molecule of O_3. Clear effect of SO_2 on ozonesonde measurements in the continental Europe was reported by Flentje et al. (2010) during the major eruption

AMTD
7, 293–320, 2014

of Eyjafjallajökull, Iceland in April 2010. Using tandem ozonesondes one with an SO_2 filter and the other without, Morris et al. (2010) determined the vertical profiles of O_3 and SO_2 simultaneously in Houston USA in the presence of industrial SO_2 plumes, and in Sapporo, Japan in the presence of volcanic SO_2 plumes.

Around MCMA, there are two major sources of SO_2: the Tula industrial complex and the Popocatépetl volcano. The Tula industrial complex has an oil refinery and an electric power plant. Popocatépetl is an active strato volcano with increased frequency of major eruptions in recent years. The impact of these SO_2 sources on the air-quality in MCMA was analyzed by de Foy et al. (2009) using ground-based monitoring equipment, wind profilers, satellite remote sensing, and numerical chemical transport models. They identified frequent ground-level high SO_2 incidents with the emission from the Tula complex, and less frequent incidents with the Popocatépetl emission. However, their analysis on the contribution of the Popocatépetl relied heavily on the chemical transport model and satellite remote sensing, the former having considerable uncertainty in the complex terrain of the Valley of Mexico and the latter lacking sufficiently high spatial and temporal resolutions. There have been virtually no observations of the vertical structure of the SO_2 plumes from the two sources comparable to the observations by Morris et al. (2010). (As described later, Ozonesonde data used in Thompson et al. (2008) clearly indicate interference by SO_2, but no discussion was provided in their paper.)

In our research project "Joint Research Project on Formation Mechanism of Ozone, VOCs, and $PM_{2.5}$ and Proposal of Countermeasure Scenarios", ozonesonde measurements (without SO_2 filters) were conducted in November 2011 and March 2012 in MCMA with a principal aim of understanding the O_3 life cycle. Incidentally, in some of the measurements, we found interference to the O_3 sensor by SO_2 plumes from the two major sources around MCMA. This paper describes the observation and analysis using an atmospheric dispersion model.

AMTD
7, 293–320, 2014

2 Preliminaries

2.1 ECC ozone sensor

In our ozonesonde system, we used the Electrochemical Concentration Cell (ECC) ozone sensor (EnSci Co.). The ECC sensor consists of anode and cathode cells: the cathode cell contains buffered 0.5 % KI solution, and the anode cell saturated KI solution. The ambient O_3 is pumped at a specified volume flow rate into the cathode cell where O_3 reacts with the iodide ion (I^-) as

$$O_3 + 2H^+ + 2I^- \rightarrow I_2 + H_2O + O_2 \quad (1)$$

Through the ion bridge that connects the cathode and anode cells, the iodide ion is supplemented from the anode cell, and through the platinum electrodes inserted at the bottom of the cells, electrons flow to re-establish charge balance. The measured electric current is therefore proportional to the rate of influx of O_3 molecules.

If there is SO_2 in the ambient air, the cathode-cell reaction is modified as follows (Schenkel and Broder, 1982). First, the dissolved SO_2 dissociates into HSO_3^- and SO_3^{2-}:

$$SO_2 + H_2O \leftrightharpoons HSO_3^- + H^+ \quad (2)$$

$$HSO_3^- \leftrightharpoons SO_3^{2-} + H^+ \quad (3)$$

At pH = 7, the aqueous concentrations of HSO_3^- and SO_3^{2-} are approximately the same (Seinfeld and Pandis, 2006). Then, the dissolved O_3 reacts preferentially with these S(IV) species rather than with I^-.

$$O_3 + HSO_3^- \rightarrow SO_4^{2-} + O_2 + H^+ \quad (4)$$

$$O_3 + SO_3^{2-} \rightarrow SO_4^{2-} + O_2 \quad (5)$$

AMTD
7, 293–320, 2014

Because these reactions do not induce electric current through the electrodes, the current that would have resulted from the iodide-ozone reaction is lost. In other words, 1 molecule of SO_2 is measured as −1 molecule of O_3. If there are more SO_2 molecules than O_3 molecules, the unreacted HSO_3^- and SO_3^{2-} remains in the aqueous phase until all is consumed by the later incoming O_3. In the measurement, this means that zero signal continues until all the dissolved SO_2 is consumed. As explained in Schenkel and Broder (1982), reaction of O_3 with the dissolved forms of NO_x is not preferred over that with I^-.

To prevent the SO_2 interference, strong oxidizing agent is used to filter out SO_2 in KI-based O_3 monitors. Morris et al. (2010) demonstrated application of CrO_3-based SO_2 filter to ECC ozone sensors. Using two ECC sensors in tandem, one with the SO_2 filter and the other without, they could measure O_3 and SO_2 concentrations simultaneously. In our observation campaigns, we did not apply the SO_2 filter because at the time of campaign planning we were not aware of the SO_2 interference or the filtering technology.

A property of ECC sensor that is helpful in interpreting the observed signal is the response time to a sudden change of input-gas composition. We conducted a laboratory experiment where the input gas was switched between ozone-free air and ozone-containing air (about 160 ppb). For eight ECC sensors, the output current could be fitted approximately to exponential forms

$$I = I_b + (I_0 - I_b)(1 - \exp(-t/\tau_r)) \text{ (rise response)}, \quad (6)$$

$$I = I_b + (I_0 - I_b)\exp(-t/\tau_d) \text{ (decay response)}, \quad (7)$$

where $I_0 = 5.0\,\mu A$ is the ECC output for the ozone-containing air, $I_b = 0.3\,\mu A$ is the background current for the ozone-free air, and time constants are $\tau_r \approx 22\,s$ and $\tau_d \approx 21\,s$.

Figure 2 shows the response of the sensor output when the input gas was changed from ozone-containing air (about 160 ppb) to ozone-free air, 200 ppb SO_2-containing air, 200 ppb NO-containing air, or a mixture of 200 ppb NO and 150 ppb O_3 air. The last gas was used to examine the response to NO_2 that results from the reaction between

AMTD
7, 293–320, 2014

NO and O_3. Because SO_2 dissolves quickly into the solution and prevents residual O_3 from reacting with I^-, the response to SO_2 was much faster than that to other gases.

2.2 SO_2 sources

There are two major sources of SO_2 around MCMA: the Tula industrial complex and the Popocatépetl volcano (see Fig. 1). In the Tula industrial complex (20°03′ N, 99°17′ W) located about 70 km to northwest of our observation site at Servicio Meteorologico Nacional (SMN), the SO_2 emission is mostly from the Miguel Hidalgo oil refinery and Francisco Pérez Ríos power plant, the former emitting 76 $kt\,yr^{-1}$ and the latter 136 $kt\,yr^{-1}$ according to the 2008 version of National Inventory of Emissions in Mexico (INEM2008 compiled by SEMARNAT). In contrast, the SO_2 emission in the Federal District, the core area of MCMA, is 2.8 $kt\,yr^{-1}$, of which about 2.0 $kt\,yr^{-1}$ is from mobile sources. Hence, it is only 1.3 % of that from the Tula complex.

The emission from the Tula complex is not steady, and the ambient SO_2 measured at the monitoring stations in the northern part of MCMA show irregular intermittent peaks often reaching as high as 300 ppb. Figure 3 shows histograms of hourly SO_2 concentrations at Villa de las Flores (VIF), Pedregal (PED), and Chalco (CHO) monitoring stations (see Fig. 1) in the RAMA (Spanish acronym for automatic atmosphere monitoring network) network for the period from 1 January to 31 December 2011. We observe that the frequency of high concentration increases as the station becomes closer to the Tula complex.

Popocatépetl (5426 m a.s.l., 19°01′20″ N, 98°37′40″ W) is an active strato volcano located about 70 km southeast of SMN. It has been virtually dormant from 1927 to 1994, when an ash emission occurred, but since December 2000, when large eruptions happened, has been degassing continuously and erupting sporadically. The rate of SO_2 emission was estimated at 2.45±1.39 $kt\,day^{-1}$ (894±507 $kt\,yr^{-1}$) by Grutter et al. (2008) based on DOAS measurement in March 2006. Although the estimated emission rate is considerably larger than that from the anthropogenic sources, the contribution to the

AMTD
7, 293–320, 2014

ground-level concentration is relatively small because the height of emission is above or approximately equal to the top of the convective boundary layer. de Foy et al. (2009) estimated, by numerical simulation models, the contribution at 3–18 % in March 2006 when the MILAGRO campaign was conducted.

2.3 Ozonesonde observation

With the aim of unraveling the life cycle of O_3 in MCMA, we conducted ozonesonde observation in November 2011 and March 2012. The balloon launch site was the rooftop of the SMN building (2313 m a.s.l., 19°24′13″N, 99°11′46″W, WMO station index 76 679) where routine atmospheric sounding is conducted twice daily at 00Z and 12Z (18:00 and 06:00 LST, respectively). The observation dates were 17, 22, 23 November 2011, and 7, 8, 9, 12, 13, 14 March 2012. On each day, GPS radiosonde (Meisei Electric, Co. Ltd.) was launched at 08:30 and 17:30, and ozonesonde (GPS radiosonde + ECC O_3 sensor (EnSci Co.)) at 11:30 and 14:30, where the time is in LST. The actual balloon launching times were often later than these nominal times by up to 30 min. The rate of climb of the observation balloons was set at about 5 m s^{-1}, and the data were recorded up to about 15 km for the GPS radiosonde and 30 km for the ozonesonde until the balloon burst. In this paper, we present results up to 8 km a.s.l. below which SO_2 interference to the ECC sensor was observed. Results at higher altitudes and characteristics regarding ozone life cycle will be presented elsewhere.

At the launching site, we installed an O_3 monitor based on UV absorption (OA-781, Kimoto Electric) for all the observation periods and an SO_2 monitor based on UV absorption (Model 43C, Thermo Scientific) on 12–14 March 2012. They provided the ground-level ambient concentrations.

AMTD
7, 293–320, 2014

3 SO_2 interference events

3.1 Popocatépetl emission

During the campaign of November 2011, sudden drops of the ECC sensor output were observed frequently at about 5 km a.s.l. Figure 4 shows the vertical profiles of the partial pressure of O_3 for conspicuous cases: one or two sharp minima for the launches at 14:30 17 November, 11:30 22 November, and 11:30 23 November, and about 1.5 km-thick layer of zero signal for the launch at 14:30 22 November. Outside the minima region, the signal magnitude and fluctuation appeared normal, and the ground-level concentration of O_3 by the ECC sensor agreed well with that measured by the UV-based equipment. We remark that the concerned range of the sounding profiles can be regarded as the vertical profiles at SMN because the horizontal travel distance of the observation balloons until they rose to 8 km a.s.l. was at most 7 km from SMN.

The sudden changes in the ECC sensor signal cannot be explained by sudden changes in the ambient O_3 concentration. The dashed curves in Fig. 4 indicate the response of the ECC sensors if the ambient O_3 partial pressure was assumed to drop abruptly to zero from the values at the bottom of the curves. Except for the case 11:30 23 November, the assumed response curves are more gradual than the observed curves.

A probable cause of the sudden signal drops is SO_2 plumes from Popocatépetl. As shown in Sect. 2.1, presence of SO_2 reduces the sensor output at a much faster rate than the other tested gases including ozone-free air. The summit crater of Popocatépetl is at about the same height as the signal drops. During the observation campaign, Popocatépetl was relatively active with a large eruption on 20 November. Our sounding results show that the wind was generally from the southeast around the height of Popocatépetl summit so that the emitted SO_2 from Popocatépetl could be advected toward SMN.

Emission of NO_x from airplanes was also a concern because the flights coming to and leaving from the Mexico City international airport passed over SMN very frequently

AMTD
7, 293–320, 2014

(almost every few minutes). However, as demonstrated by Schenkel and Broder (1982) and by our experiment (Fig. 2), NO_x has negligible effect on the ECC ozone sensor.

In the case of 14:30 22 November (Fig. 4c), it can be inferred either that the SO_2 plume had thickness of about 1.5 km or that the concentration of SO_2 was higher than O_3 at a certain height so that zero signal continued until the residual S(IV) ions in the reaction cell were consumed. Whether the SO_2 plume could have thickness comparable to the affected layer ($\approx$ 1.5 km) is examined later by numerical simulation. We note that the time required for an air parcel to travel from Popocatépetl to SMN was 2–4 h because the wind speed was in the range of 5–10 m s^{-1}. Because there was no report of large eruptions on the day, the plume should have been due to passive degassing from the crater.

For the cases where the signal did not hit zero, the signal profiles indicate the vertical structures of the SO_2 plumes. They do not necessarily indicate the dominant thickness of the plumes because the observation balloons could have moved through the fringe regions of the plumes. For the same reason and also because the emission rate from Popocatépetl is unknown, the overall concentration field of the SO_2 plumes is difficult to estimate merely from the observed signals. Despite these limitations, we can at least say from Fig. 4 that the plume thickness was larger than a few hundred meters.

To evaluate the thickness of the Popocatépetl SO_2 plume, numerical simulation was conducted using WRF v.3.3.1 (Skamarock et al., 2008) and FLEXPART (Stohl et al., 2005) that was modified to work with WRF outputs (Fast and Easter, 2006). Salient conditions of the simulation were as follows. In the WRF simulation, a single domain was defined around Popocatépetl with 288 × 186 × 32 grids of 3 km × 3 km horizontal size. The thickness of the 32 layers increased from 26 m at the bottom to about 600 m near 3 km a.g.l. and above up to the domain top at 16 km a.s.l. The input meteorological data were NCEP final reanalysis (FNL) with 1° × 1° horizontal resolution and 6 h time interval. The spatial resolution of the terrain data was 30 s. The sub-models employed were WSM 6-class model for cloud microphysics, MM5 Monin–Obukhov model for the surface boundary layer, Yonsei University model for the planetary boundary layer, and

AMTD
7, 293–320, 2014

the unified Noah model for the land surface. Because the FNL data did not resolve the fine structure of the wind field as obtained by our sounding, observation nudging was applied to the whole domain using our sounding data conducted four times during daytime. Grid nudging (typical data assimilation technique when additional observation data are not available) was also applied at the times when the FNL data were available. These nudging procedures in effect introduced non-physical forcing to the governing equations in the whole domain well beyond the valid range of the sounding results, but for the current purpose of reproducing the approximate SO_2 plume, this rather crude method can be justified. The WRF simulation was run for 48 h from 00:00 (UTC) of 21 November 2011, the first 24 h considered as a spin-up period.

A Lagrangian stochastic model FLEXPART was employed because the steep terrain near Popocatépetl would induce substantial numerical diffusion if an Eulerian diffusion model were used. The basis wind field was the WRF simulation results saved at 1 h intervals. Above the Popocatépetl crater in the a.s.l. height range between 5426 (summit) and 5926 m, a total of one million particles were released randomly for 20 h starting at 01:00 (UTC) on 22 November 2011.

Figure 5a compares the wind speed and direction of the WRF simulation and the sounding result for 21:00 UTC (15:00 LST) on 22 November 2011. We observe that the west to south-west wind around 6 km a.s.l. is reproduced fairly well. Note that, without observation nudging, the wind direction variation from 4 to 8 km could not be reproduced and the simulated wind was almost uniformly from the west.

Figure 5b shows the concentration contour at 5500 m a.s.l. at 21:00 UTC (15:00 LST) on 22 November 2011. The blue dot indicates the location of SMN. The plume is transported primarily toward west but some portion is carried to the north-west where SMN is located. As shown in Fig. 5a, the observed wind had more south-westerly component, and the real plume should have been bent further toward the north than in Fig. 5b.

Figure 5c shows the vertical profile of the number of particles in the range of horizontal radial distance from 60 to 80 km from Popocatépetl. The number of particles is normalized by the maximum value around 5500 m a.s.l. The profile indicates that the

AMTD
7, 293–320, 2014

plume thickness is about 1 km. The thickness was almost the same for other times and under other similar simulation conditions (e.g., different release height) not considerably different from the presented case. Therefore, for the interpretation of the case shown in Fig. 4c, corresponding to the simulation time of Fig. 5, there still remains two possibilities, i.e., the sounding balloon either transected a thick portion of the plume, or met a thin but dense-SO_2 portion of the plume and the ECC sensor was interfered continuously until all the dissolved SO_2 molecules were consumed. In other cases of Fig. 4, the balloons may have traversed thin portions such as at the fringe of the plume.

3.2 Tula emission

On 14 March 2012, the 11:30 launch of ozonesonde experienced a considerably lower reading (≈ 33 ppb) of O_3 than the UV-based equipment (≈ 53 ppb). As shown in Fig. 6, the vertical profile of O_3 concentration had a considerably thicker layer of reduced O_3 than those of typical launches for which the near-ground reduction was due to decomposition on solid surfaces and reaction with NO. The ground-level O_3 concentration on 14 March was relatively low with an afternoon maximum of about 65 ppb. Otherwise, it was a fine day with no abnormal meteorological phenomena.

There are circumstantial evidence that suggests the reduced O_3 reading was due to SO_2 plume from the Tula industrial complex. Figure 7 shows the SO_2 and O_3 concentrations measured by the UV-based equipment at SMN and at a nearby monitoring station PED (see Fig. 1) on 14 March. From wee hours to shortly after the 11:30 launching, the SO_2 monitors captured sporadic large peaks of SO_2. At the time of balloon release (note that 11:30 is a nominal time, and the actual release time was 11:54), the SO_2 concentration was about 21 ppb, approximately the same magnitude as the difference between the ozonesonde reading and the measurement by the UV-based O_3 monitor. The wind direction was from the north in the morning hours, and the SO_2 concentration in the north-western part of Mexico City was generally higher than usual and than other parts. The Vallejo district in the north of SMN is also a large emission source of SO_2,

AMTD
7, 293–320, 2014

but all the three air-monitoring stations (ATI, TLI, and VIF) in the north of the Vallejo district recorded sporadic high SO_2 concentration in the same period.

An instantaneous plume was simulated by WRF+FLEXPART employing grid and observation nudging described previously. The effective stack height of the Tula emissions was estimated to be in the range from 400 to 1430 m by substituting the properties of the individual stacks provided in INEM2008 into the CONCAWE relation (Brummage, 1968). Then, in the height range between 100 and 1000 m a.g.l., one million particles were released randomly for 20 h starting at 01:00 (UTC) on 14 March 2012. Figure 8 shows the concentration contour at 2500 m a.s.l. at 12:00 LST on 14 March. The simulated plume traveled primarily toward the south although the observed surface SO_2 distribution obtained from the RAMA stations indicated plume advancement toward the south-east (not shown). It should be noted that the plume traveled mainly to the west if the observation nudging based on our sounding results was not employed. Because presence of one-molecule SO_2 is detected as absence of one-molecule O_3 by the ECC sensor, the output signal C_{ECC} of the ECC sensor when the ground-level SO_2 concentration is 21 ppb and O_3 concentration is 53 ppb becomes

$$C_{ECC} = 53 - 21\frac{C_{SO_2}(z)}{C_{SO_2}(0)}. \quad (8)$$

The vertical profile of SO_2 concentration at SMN (average of 11:00 and 12:00 LST results) was substituted in Eq. (8), and the result is shown by the thick green line in Fig. 6. The calculated profile agrees well with the observation except near the ground where the gradient is a little excessive. We note that a plume simulation using a conventional Gaussian-plume method resulted in a poorer agreement with the observation (not shown) probably because this method cannot account for the complex evolution of the boundary layer in the morning hours while the plume traveled from the Tula complex to SMN for about 6.5 h.

AMTD
7, 293–320, 2014

4 Assessment of SO_2 influence on ozonesonde

4.1 Effect of Popocatépetl plume

We identify the season when ozonesonde observation is most likely to be interfered by the SO_2 plume from Popocatépetl. For this purpose, the wind vectors measured by the routine soundings at 00Z and 12Z from SMN are averaged vector-wise in the height range from the Popocatépetl summit to 1000 m above the summit (5426–6426 m a.s.l.). The raw data of the routine soundings (using Vaisala GPS radiosondes) containing measured values at every two seconds (approximately 9-m interval) were provided by SMN. The directions of the vertically averaged wind vectors were sorted into bins of 16 compass-point directions, and the frequency distributions were determined for given time periods. The compilation period was from 2006 to 2010, and months with similar distributions were lumped together. Both 00Z and 12Z data were averaged together because diurnal variation was relatively weak at the concerned altitudes. Figure 9 shows the result.

The prevailing wind direction is W from November to March; E from June to September; and intermediate between these groups of months, i.e., in May and October. The change of wind directions reflects the alternation of the thermal wind. Because Mexico City is located to the northwest of Popocatépetl, ECC ozonesonde would be frequently affected by the Popocatépetl SO_2 plume from June to October when the frequency of SE wind is high (≥ 8 %). Our encounter with the Popocatépetl interference in November is due to meteorological variability; the wind direction in the upper troposphere was indeed not constant (WSW on 17 November, E on 22 and 23 November), typical of transition period from the wet to dry season.

If SO_2 filters (Morris et al., 2010) are to be employed to avoid Popocatépetl interference in the future routine ozonesonde observations, it would be sufficient to use them in months from June to October.

AMTD
7, 293–320, 2014

4.2 Effect of Tula plume

As described in Whiteman et al. (2000), solar heating of the ground and the induced updraft in the Mexico Basin generates relatively weak surface air-flow from the wide orographic opening to the north (see Fig. 1). Therefore, the prevailing wind is from the north in most of MCMA except in the southeastern part where strong wind enters in the afternoon from the narrow gap of the basin rim in the south-east corner.

Because the surface observation could be influenced by the surrounding buildings, we analyzed the average wind direction measured by the routine soundings in the height range from 2343 to 2463 m a.s.l., i.e., up to 150 m a.g.l. excluding the first 30 m. Figure 10 shows the averaged wind-direction frequency from 2006 to 2010. There were variations from year to year (not shown), but the common characteristics is that the prevailing wind direction is N at 00Z and NW-NNW at 12Z. Therefore, the wind is frequently from the Tula complex to the center of Mexico City. As shown in Fig. 3, high-SO_2 plume is not very frequent, but when it occurs, it almost certainly reaches the SMN site and affects the ozonesonde observation. In our measurement campaigns, 1 in 18 launches was interfered by the Tula plume.

Therefore, some countermeasure should be implemented against SO_2 interference. Probable measures are employing SO_2 filters on all the ECC sensors, monitoring SO_2 concentration at the launching site to avoid high-SO_2 events, or preventing the sporadic large emissions of SO_2 from the Tula complex; the last option is of course beneficial to the air quality in MCMA.

5 Conclusions

In the ozonesonde observations during our atmospheric research campaign in Mexico City, we found abnormal drops in the ECC sensor signal around and above 5 km a.s.l. (17, 22, 23 November 2011) or in the convective boundary layer (14 March 2012). Analysis of the sensor response time, the emissions inventory, the weather condition,

AMTD
7, 293–320, 2014

and plume dispersion simulations indicates that the drops in the signal were caused by SO_2 interference by plumes from the Popocatépetl volcano (17, 22, 23 November 2011) and the Tula industrial complex (14 March 2012). From the analysis of the wind-field statistics in the Valley of Mexico, we expect that there would be frequent interference by the Popocatépetl plume from June to October and by the Tula plume whenever large emission occurs.

If, in future, regular ozonesonde observations are to be conducted in Mexico City, SO_2 filter will have to be installed at times when interference by SO_2 plumes are expected. Also, the emission of SO_2, which is a health hazard by itself and a precursor to fine particulate matter (another health risk), from the Tula complex should be reduced to improve the air quality.

Acknowledgements. This work was conducted as part of "Joint Research Project on Formation Mechanism of Ozone, VOCs, and $PM_{2.5}$ and Proposal of Countermeasure Scenarios" under the SATREPS scheme funded by Japanese agencies JST and JICA. We are grateful to SEMARNAT of Mexico for providing the source data of INEM 2008. We appreciate the assistance of the technicians from Mexican institutes during the sounding campaigns, Moe Izumi at Ehime University for the ECC-sensor response experiments, and Armando Retama from the Ministry of Environment of the Mexico City government for providing information on major contributors to the SO_2 concentration in Mexico City.

References

Brummage, K. G.: The calculation of atmospheric dispersion from a stack, Atmos. Environ., 2, 197–224, 1968. 305

de Foy, B., Krotkov, N. A., Bei, N., Herndon, S. C., Huey, L. G., Martínez, A.-P., Ruiz-Suárez, L. G., Wood, E. C., Zavala, M., and Molina, L. T.: Hit from both sides: tracking industrial and volcanic plumes in Mexico City with surface measurements and OMI SO_2 retrievals during the MILAGRO field campaign, Atmos. Chem. Phys., 9, 9599–9617, doi:10.5194/acp-9-9599-2009, 2009. 296, 300

Emmons, L. K., Apel, E. C., Lamarque, J.-F., Hess, P. G., Avery, M., Blake, D., Brune, W., Campos, T., Crawford, J., DeCarlo, P. F., Hall, S., Heikes, B., Holloway, J., Jimenez, J. L.,

AMTD
7, 293–320, 2014

Knapp, D. J., Kok, G., Mena-Carrasco, M., Olson, J., O'Sullivan, D., Sachse, G., Walega, J., Weibring, P., Weinheimer, A., and Wiedinmyer, C.: Impact of Mexico City emissions on regional air quality from MOZART-4 simulations, Atmos. Chem. Phys., 10, 6195–6212, doi:10.5194/acp-10-6195-2010, 2010. 295

Fast, J. D. and Easter, R. C.: A Lagrangian particle dispersion model compatible with WRF, 7th Annual WRF User's Workshop, 19–22 June 2006, Boulder, CO, USA, 2006. 302

Flentje, H., Claude, H., Elste, T., Gilge, S., Köhler, U., Plass-Dülmer, C., Steinbrecht, W., Thomas, W., Werner, A., and Fricke, W.: The Eyjafjallajökull eruption in April 2010 – detection of volcanic plume using in-situ measurements, ozone sondes and lidar-ceilometer profiles, Atmos. Chem. Phys., 10, 10085–10092, doi:10.5194/acp-10-10085-2010, 2010. 295

Grutter, M., Basaldud, R., Rivera, C., Harig, R., Junkerman, W., Caetano, E., and Delgado-Granados, H.: SO_2 emissions from Popocatépetl volcano: emission rates and plume imaging using optical remote sensing techniques, Atmos. Chem. Phys., 8, 6655–6663, doi:10.5194/acp-8-6655-2008, 2008. 299

Loyola, D., van Geffen, J., Valks, P., Erbertseder, T., Van Roozendael, M., Thomas, W., Zimmer, W., and Wißkirchen, K.: Satellite-based detection of volcanic sulphur dioxide from recent eruptions in Central and South America, Adv. Geosci., 14, 35–40, doi:10.5194/adgeo-14-35-2008, 2008.

Mage, D., Ozolins, G., Peterson, P., Webster, A., Orthofer, R., Vandeweerd, V., and Gwynne, M.: Urban air pollution in megacities of the world, Atmos. Environ., 30, 681–686, 1996. 294

Morris, G. A., Komhyr, W. D., Hirokawa, J., Flynn, J., Lefer, B., Krotkov, N., and Ngan, F.: A balloon sounding technique for measuring SO_2 plumes, J. Atmos. Ocean. Tech., 27, 1318–1330, 2010. 296, 298, 306

Schenkel, A. and Broder, B.: Interference of some trace gases with ozone measurements by the KI method, Atmos. Environ., 16, 2187–2190, 1982. 297, 298, 302

Seinfeld, J. H. and Pandis, S. N.: Atmospheric Chemistry and Physics, From Air Pollution to Climate Change, John Wiley & Sons, Inc., New Jersey, 2006. 295, 297

Skamarock, W. C., Klemp, J. B., Dudhia, J., Gill, D. O., Barker, D. M., Duda, M. G., Huang, X.-Y., Wang, W., and Powers, J. G.: A description of the Advanced Research WRF Version 3, NCAR/TN-475+STR, 2008. 302

Stohl, A., Forster, C., Frank, A., Seibert, P., and Wotawa, G.: Technical note: The Lagrangian particle dispersion model FLEXPART version 6.2, Atmos. Chem. Phys., 5, 2461–2474, doi:10.5194/acp-5-2461-2005, 2005. 302

AMTD
7, 293–320, 2014

Thompson, A. M., Yorks, J. E., Miller, S. K., Witte, J. C., Dougherty, K. M., Morris, G. A., Baumgardner, D., Ladino, L., and Rappenglück, B.: Tropospheric ozone sources and wave activity over Mexico City and Houston during MILAGRO/Intercontinental Transport Experiment (INTEX-B) Ozonesonde Network Study, 2006 (IONS-06), Atmos. Chem. Phys., 8, 5113–5125, doi:10.5194/acp-8-5113-2008, 2008. 295, 296

Velasco, E., Márquez, C., Bueno, E., Bernabé, R. M., Sánchez, A., Fentanes, O., Wöhrnschimmel, H., Cárdenas, B., Kamilla, A., Wakamatsu, S., and Molina, L. T.: Vertical distribution of ozone and VOCs in the low boundary layer of Mexico City, Atmos. Chem. Phys., 8, 3061–3079, doi:10.5194/acp-8-3061-2008, 2008. 295

Whiteman, C. D., Zhong, S., Bian, X., Fast, J. D., and Doran, J. C.: Boundary layer evolution and regional-scale diurnal circulations over the Mexico Basin and Mexican plateau, J. Geophys. Res., 105, 10081–10102, 2000. 307

AMTD
7, 293–320, 2014

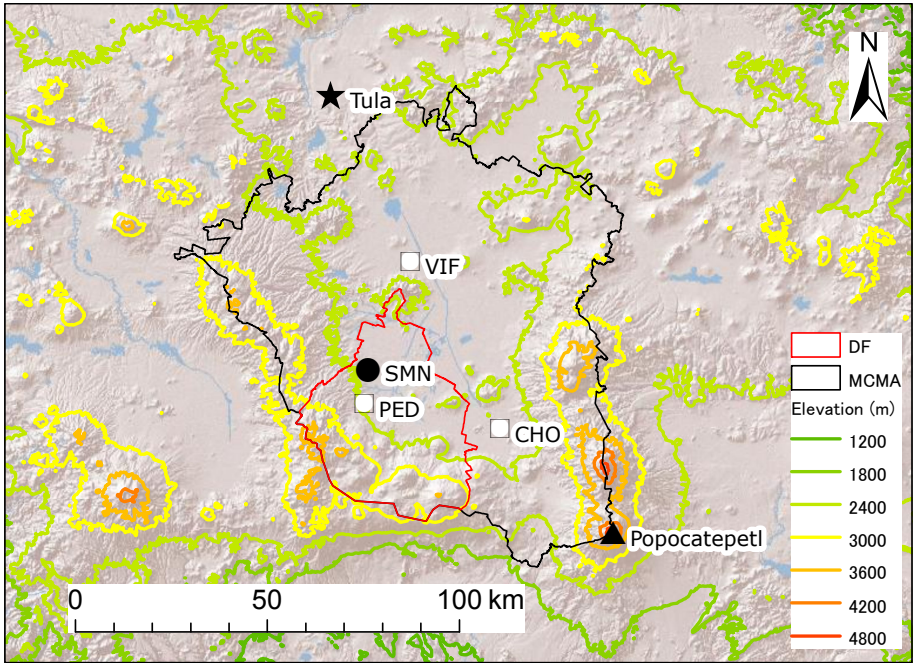

Fig. 1. Map of the Mexico City Metropolitan Area (MCMA).

AMTD
7, 293–320, 2014

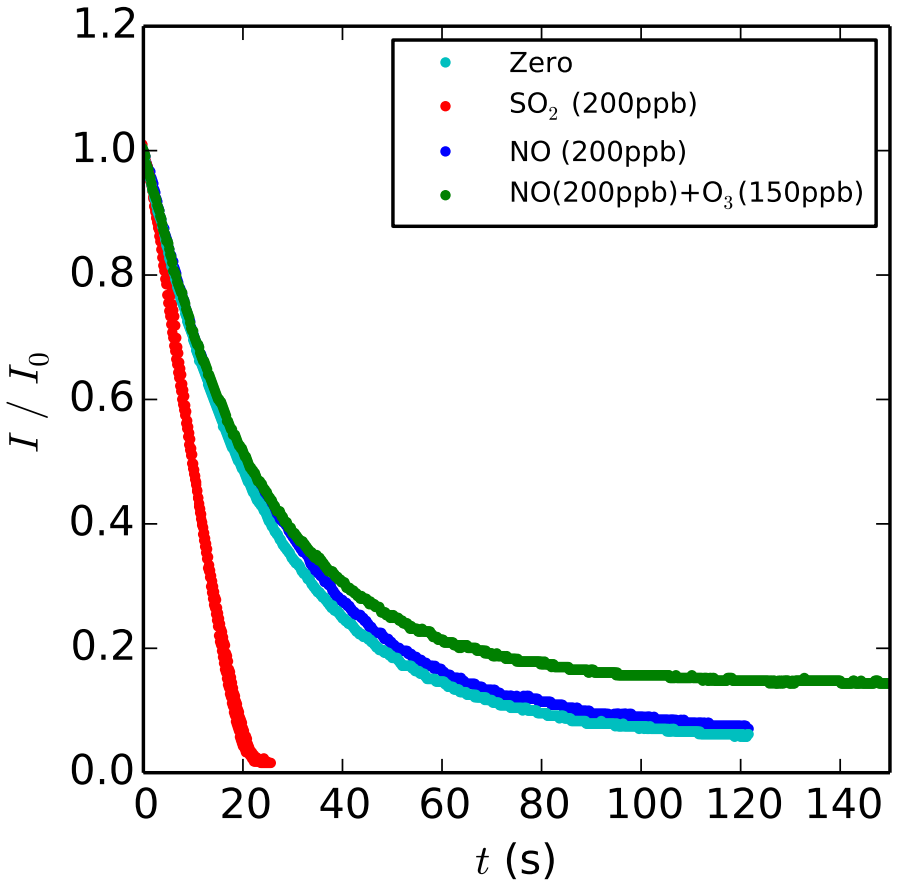

Fig. 2. Response of the ECC ozone sensor when the input gas was changed abruptly from ozone-containing air (≈ 160 ppb) to various gases indicated in the legend where "Zero" represents air filtered through activated carbon to remove ozone.

AMTD
7, 293–320, 2014

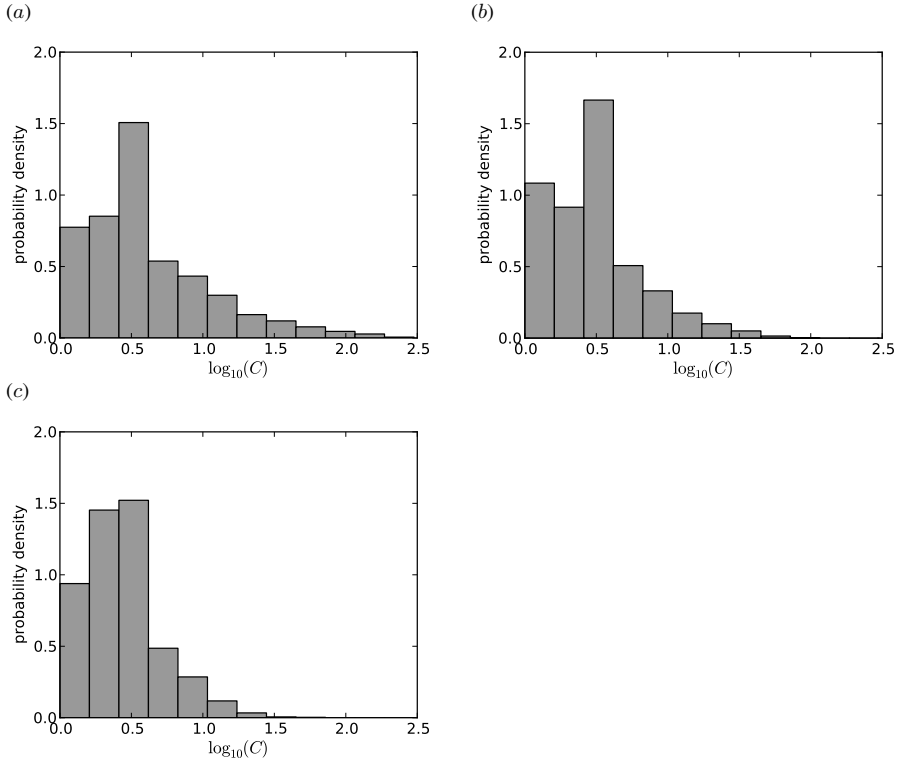

Fig. 3. Histograms (probability density distributions) of hourly SO_2 concentrations at VIF **(a)**, PED **(b)**, and CHO **(c)** stations (see Fig. 1) in the Mexico City air-monitoring network (RAMA) in the period from 1 January to 31 December 2011. The probability density f_i is defined such that $\sum_i f_i \Delta(\log_{10} C)_i = 1$, where i indicates each bin of the histogram.

AMTD
7, 293–320, 2014

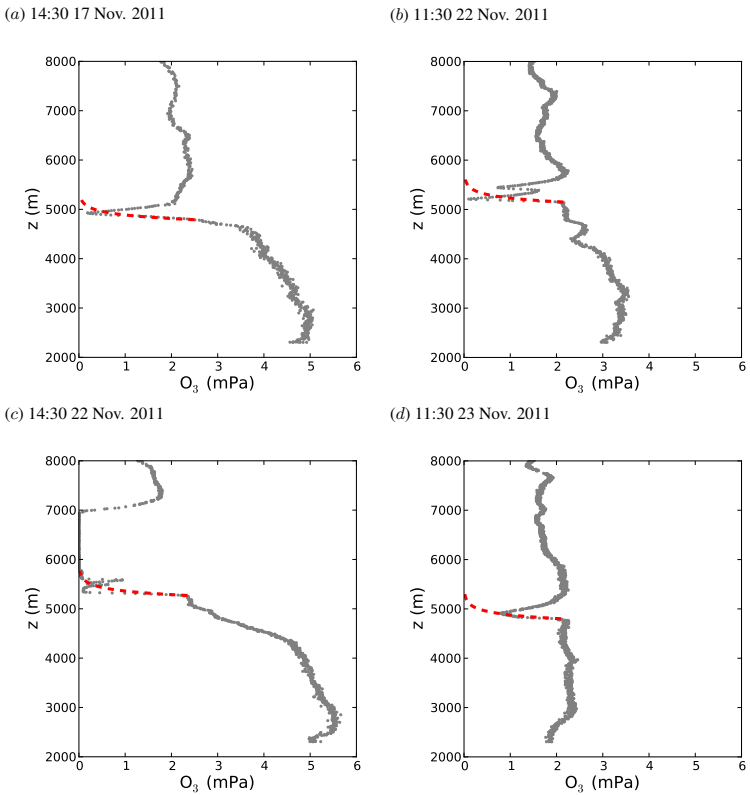

Fig. 4. Vertical profiles of the partial pressure of O_3 during the campaign in November 2011. The nominal launch times are LST. The height z is a.s.l. The dashed curves indicate expected responses of the ECC ozone sensor if the ozone concentration dropped abruptly to zero at the height corresponding to the bottom of the curves.

AMTD
7, 293–320, 2014

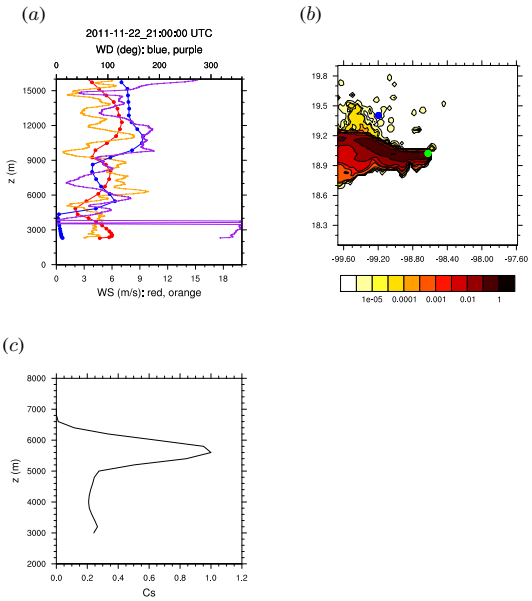

Fig. 5. Results of WRF+FLEXPART numerical simulation for 15:00 LST (21:00 UTC) on 22 November 2011. The height z is a.s.l. **(a)** Vertical profiles of wind speed (red: WRF, orange: observation) and direction (blue: WRF, purple: observation). **(b)** Forward particle dispersion simulation by FLEXPART. One million particles totaling a unit mass were released from the Popocatépetl summit for 20 h beginning at 01:00 (UTC) on 22 November 2011. The release height was between 5426 (summit) and 5926 m a.s.l. The contours represent the concentration (m^{-3}) in the horizontal section at 5500 m a.s.l. The coordinate values are longitude (positive in the east) and latitude (positive in the north) in degrees. The blue and green circles indicate the locations of SMN and the summit of Popocatépetl, respectively. **(c)** Vertical profile of the number of particles in the range of horizontal radial distance between 60 and 80 km from Popocatépetl. The particle number is normalized by the peak value at 5500 m a.s.l.

AMTD
7, 293–320, 2014

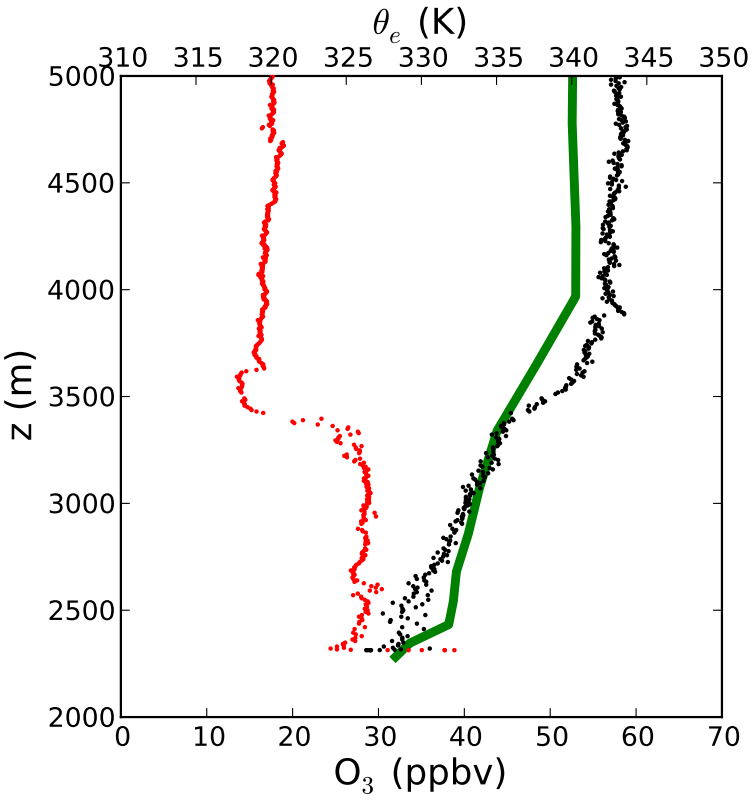

Fig. 6. Vertical distribution of O_3 concentration of the 11:30 (LST) launch on 14 March 2012. Black dots: O_3 concentration, red dots: equivalent potential temperature, and green curve: O_3 concentration influenced by the SO_2 plume (average of 11:00 and 12:00 LST results) simulated by WRF-FLEXPART.

AMTD
7, 293–320, 2014

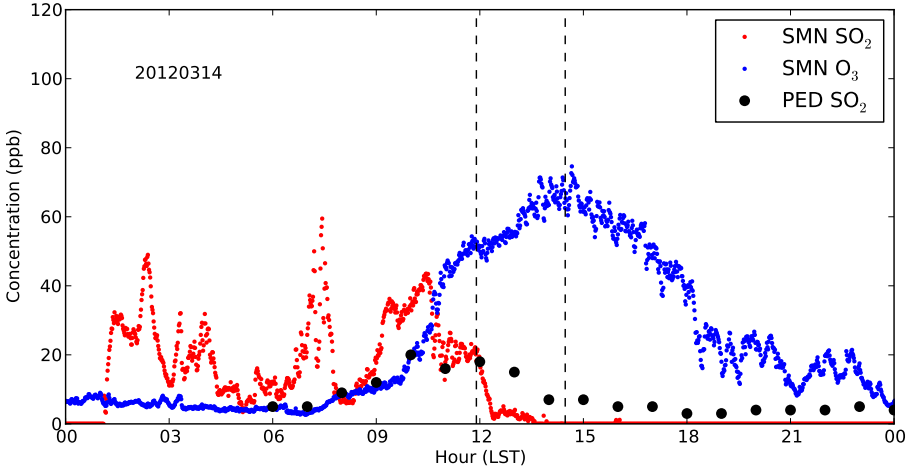

Fig. 7. Trends of O_3 and SO_2 concentrations measured by UV-based equipment at SMN and PED (SO_2 only) on 14 March 2012.

AMTD
7, 293–320, 2014

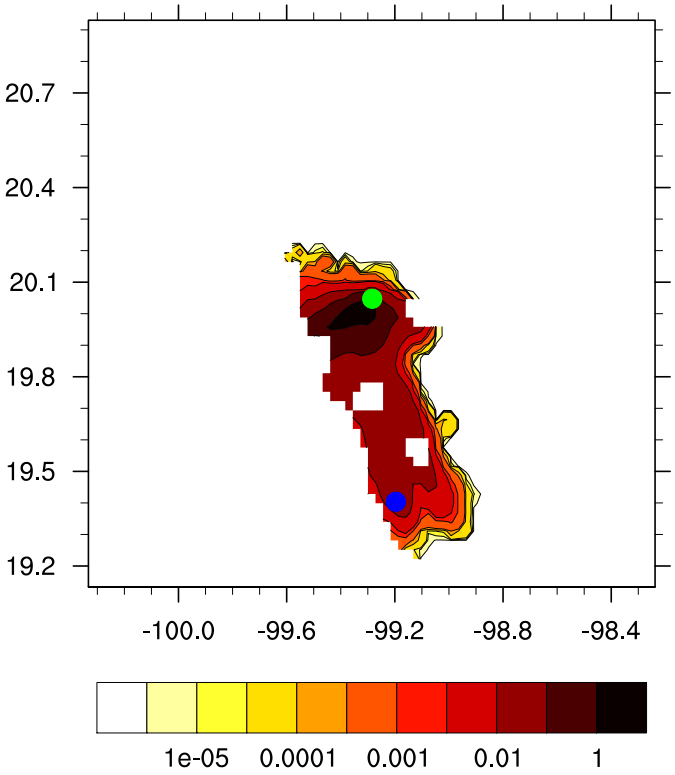

Fig. 8. Result of WRF+FLEXPART numerical simulation for 12:00 LST (18:00 UTC) on 14 March 2012. One million particles totaling a unit mass were released from the Tula industrial complex (green circle) for 20 h beginning at 01:00 (UTC) on 14 March 2012. The release height was between 100 and 1000 m a.g.l. The contours represent the concentration in the horizontal section at 2500 m a.s.l. The white defected cells indicate terrain above 2500 m a.s.l. The coordinate values are longitude (positive in the east) and latitude (positive in the north) in degrees. The blue circle indicates the location of SMN.

AMTD
7, 293–320, 2014

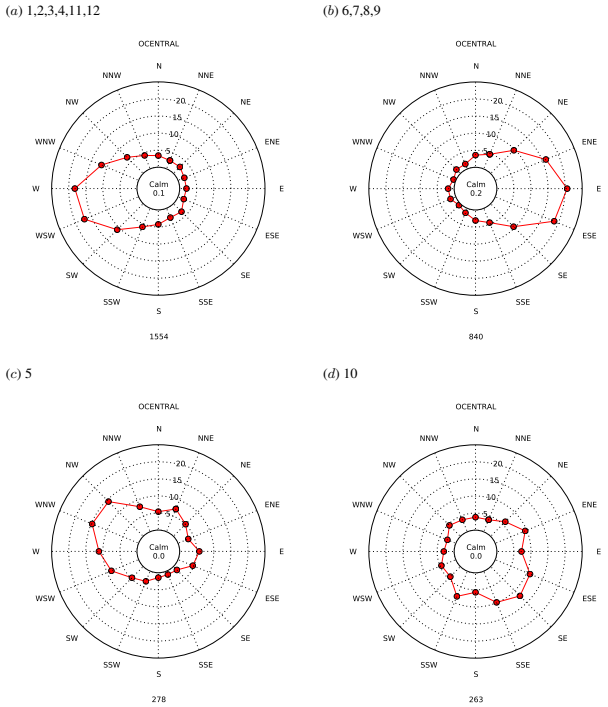

Fig. 9. Wind-direction frequency (%) distribution obtained by averaging the sounding data in the height range from the summit of Popocatépetl to 1000 m above. The data source is the routine sounding at SMN from 2006 to 2010. Months with similar distribution are grouped together: **(a)** January, February, March, April, November, and December, **(b)** June, July, August, and September, **(c)** May, and **(d)** October. The numbers at the bottom of the panels indicate the numbers of samples.

AMTD
7, 293–320, 2014

(*a*) 06 LST (12Z)

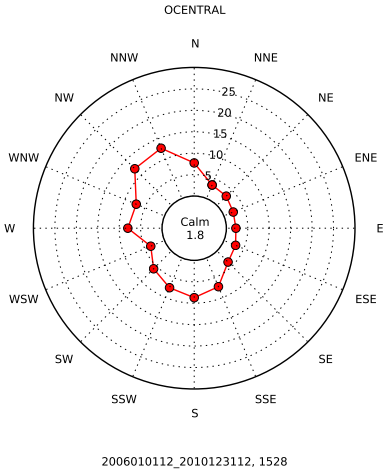

(*b*) 18 LST (00Z)

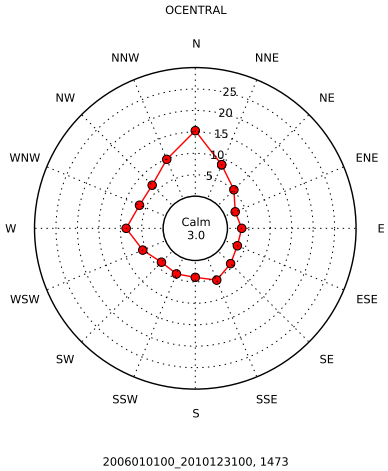

Fig. 10. Wind-direction frequency (%) distribution obtained by averaging the sounding data in the height range from 2343 to 2463 m a.s.l. (from 30 to 150 m a.g.l. at SMN). The data source is the routine atmospheric sounding at SMN from 2006 to 2010. The numbers following commas at the bottom of the panels indicate the numbers of samples.

AMTD
7, 293–320, 2014